Tropical Daylight and its Application through Window in Thailand

Pipat Chaiwiwatworakul

The Joint Graduate School of Energy and Environment, Center of Excellence on Energy Technology and Environment, King Mongkut's University of Technology Thonburi, 126 Pracha-Uthit Road, Bangmod, Tungkru, Bangkok 10140 Thailand.

Abstract: It is perceived that daylighting is a potential measure for energy conservation in commercial buildings. To success the measure implementation, comprehensive understanding of local daylight characteristic and selection of appropriate technologies are the key factors. In Thailand, a research-class daylight measuring station was established as part to promote daylighting in the country. This paper reports the investigation results of the daylight availability and sky luminance distribution patterns from the station records. A window system with movable shading slats located between two glazed panes is introduced as an effective solution of the daylight application. The simulation shows that the slat window improves the building envelope performance and reduces substantially the energy consumption from both lighting and air-conditioning.

1. Introduction

Energy use in buildings contributes significantly to national energy demand in tropical countries. In Thailand, a quarter of all electricity consumed in 2017, amounting to 45,100 GWh, is due to the commercial sector [1]. For most high-rise office buildings, their envelope comprise with large glazed windows. Adverse heat gain from solar radiation leads to the use of glazing with low visible transmittance. The practice results the buildings to full reliance on electric lighting even during the time when exterior daylight is high. Electric lighting directly shares 20% of electricity use in a building and contributes 20% of cooling load to the air-conditioning system. Air-conditioning shares 60% of electricity use, so electric lighting also contributes indirectly another 12% of electricity use through the air-conditioning system. Typical electricity consumption and power demand of an office building are 220 $kWh.m^{-2}.Y^{-1}$ and 110 $W.m^{-2}$ respectively. These figures are significant and warrant attention.

Daylighting has been studied extensively in cool climate. On the one hand, a number of stations were erected to measure daylight. The International Daylight Measurement Program (IDMP) was launch officially in 1991 to promote daylighting and to create the daylight measuring network. Availabilities of daylight illuminance have been reported from many locations since the program inception [2-5]. In addition to the daylight measurement, sky luminance distribution has been measured at some stations in Europe, USA, Japan, including Thailand [6-9].

On the other hand, research activities are being conducted to advance daylighting technologies. Different technologies with different concepts have been developed for daylighting [10]. Prismatic panels [11], holographic optical elements (HOE) [12], and anidolic zenithal opening [13] are some of the non-imaging systems that utilize diffuse skylight. Light guiding shade [14], louvers and blinds [15-16], light pipe [17-18] and light shelf [19] are the shading or redirection systems that primarily use direct sunlight. Laser cut panel [20] and thermochromic and electrochromic glass [21] are grouped into another class. Several systems are developed in order to be integrated to side window while some to be integrated on the roof.

Since 1995, Thailand regulated minimum requirements of energy performances of building systems (i.e. envelope, lighting and air-conditioning systems) of the designated buildings. The code was revised recently by strengthening the requirements and adding a new feature of accreditation of renewable energy through daylighting and photovoltaic power generation [22]. According to the code, the daylighting through side windows can be accredited in terms of the reduced light power density of the electric lighting system. The revised code was made to be effective since 2007.

An important step towards development of daylighting technology was the establishment of a station to record the daylight illuminance and sky luminance distribution. A window system with active slat control has been continuously developed to enhance the interior daylight use. In this paper, the measured results from the station were summarized that give significant insight on the character of the luminosity of tropical sky. With the available daylight data, a performance analysis of the window with the slats located between two glazed panes was carried out and presented in comparison with a typical design of heat reflective glass window.

2. Tropical Daylight

The daylight illuminances were measured for almost 20 years in Thailand. The measuring station is located in suburban area of Bangkok metropolis (latitude 14.08°N and longitude 100.62°E). The measurements include the global, diffuse horizontal and beam normal daylight illuminances. Vertical daylights on the four cardinal orientations are measured, as well. Figure 1 shows the sensors installed to measure the daylight illuminances and a sky scanner used to measure the sky luminance distribution.

(a) Daylight illuminance sensor

(b) Sky scanner

Figure 1. A daylight measuring station in Bangkok, Thailand.

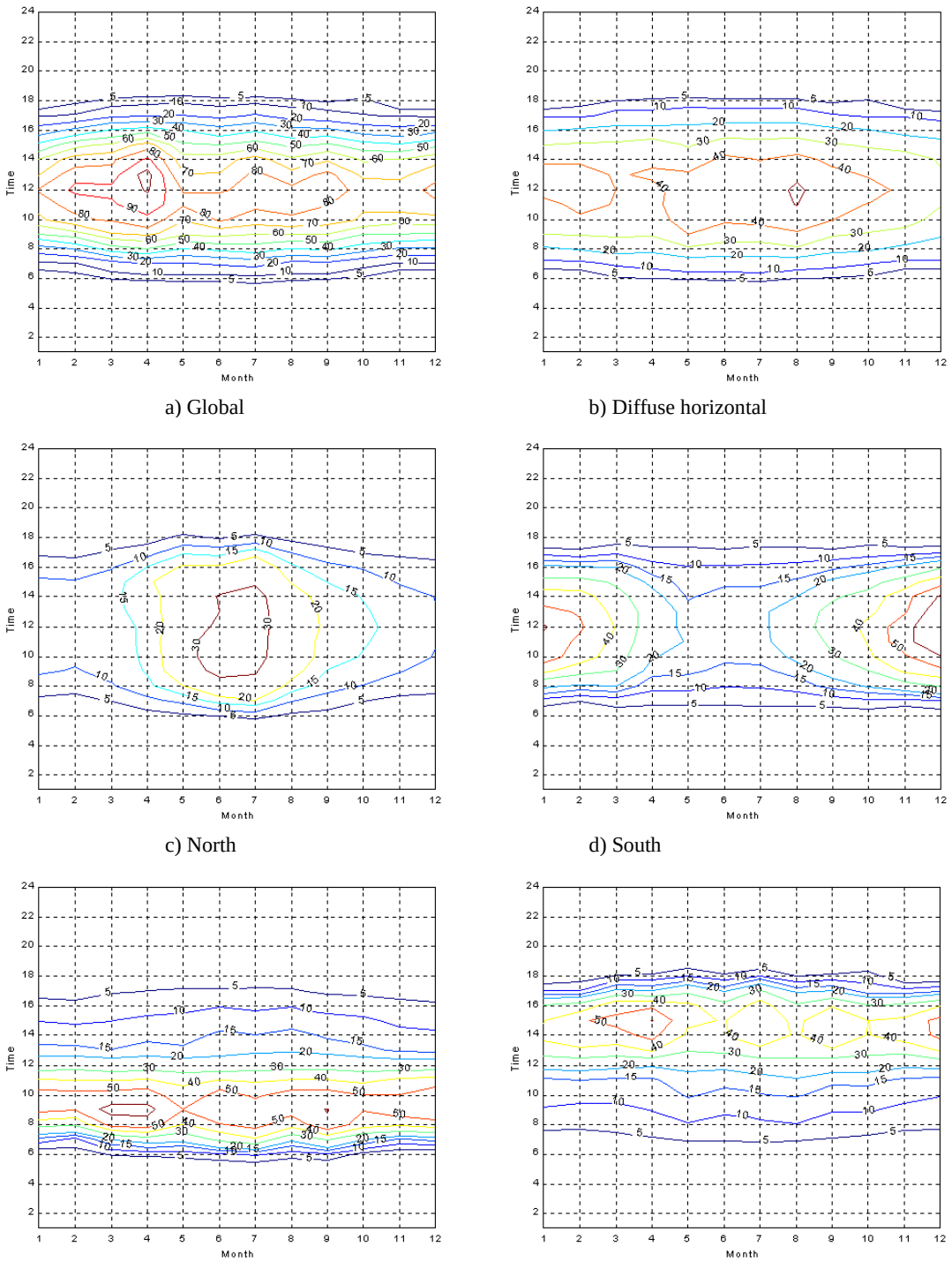

a) Global b) Diffuse horizontal

c) North d) South

e) East f) West

Figure 2. Contour plots of tropical daylight illuminance (klux).

2.1 Daylight availability

From the statistical analysis of the station records, Figs. 2(a) and (b) exhibit contour plots of the monthly average hourly values of the global and diffuse daylight illuminance with time. The main features of the plots are that the day length differs very little from month to month. The illuminance values are high throughout the year as these are expected for a tropical location, although seasonal effects can be noticed. The sky is rather clear during the cooler month of December. It remains relatively clear till April. Solar altitude reaches 90º on 27 April and 14 August. Global illuminance values are high during April, while diffuse horizontal illuminance peak in August when rain falls often and the sky is cloudy for most time.

Monthly average values of global and diffuse horizontal reach 105 and 48 klux respectively. It is noted that during office hours (8:00-16:00), the plots show that the values of global and diffuse illuminance generally exceed 20 klux. While ranges of illuminance values in Fig. 2(a) look similar to those from San Francisco [9], the higher ranges in the figure extend throughout the year instead of occurring only during the summer months in San Francisco. The ranges of diffuse illuminance in Fig. 2(b) are clearly higher than those from San Francisco and those from UK locations [10].

Figures 2(c)-(f) exhibits contour plots of total illuminance on the vertical planes of north, east, south and west orientations. The relative position of the sun with respect to each orientation clearly influences illuminance values. This influence is much more pronounced that that due to seasons. The sun remains in front of the northern direction during around May to August while for the rest of the time the sun remains in front of the southern direction and its relative position show clear effects on the plots in terms of the shift of contours of high values across those months of the year. The contour plots for the east and south directions show the effect of the position of the sun in terms of the shift of contours of thigh values between the morning and the afternoon periods. The illuminance values on the vertical planes in all orientations vary from 5 klux to a maximum of 60 klux during office hours. The patterns of variations and the ranges of values appear comparable to those obtained for San Francisco [9].

2.2 Sky luminance distribution

At the station, the luminance distribution over the sky was measured by using the sky scanner. The distribution records provide more information on the daylight characteristics. The sky scanner commences measurement of sky luminance at an altitude angle of 6° and it graduates every 12° until it reaches 90° in one scan that produces measurements of 145 points in 4.5 minutes. Figure 3 illustrates the measurement points in the sky dome in a scan and the successive altitude angles in a scan.

In 2003, the standard sky luminance distributions (SSLD) were established by the CIE as the framework for the sky classification. As exhibited in Table 1, the CIE standard categorized the distributions into fifteen types [22]. The skies no. 1-5 are categorized as overcast skies, no. 6-10 as partly cloudy skies, and no. 11-15 as clear skies.

The CIE standard set is hypothesized to encompass all possible patterns of sky distributions that may occur anywhere. It has been recommended that measurements of sky luminance at a given location be evaluated against the SSLD to determine the statistical distribution of local sky luminance distribution in terms of SSLD.

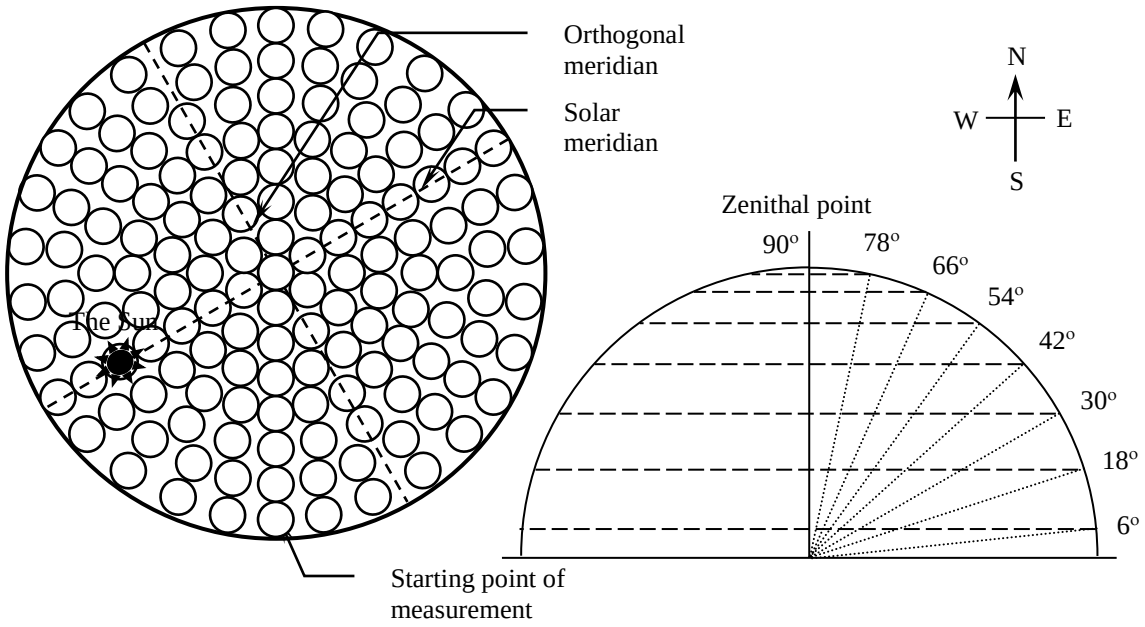

Figure 3. Measurement positions of sky luminance by sky scanner.

Table 1 Description of the fifteen CIE standard skies

No.	Sky condition	Description of sky luminance distributions
1	Overcast sky	CIE standard overcast sky, steep luminance gradation towards zenith, azimuthal uniformity
2		Overcast, with steep luminance gradation and slight brightening towards the sun
3		Overcast, moderately graded with azimuthal uniformity
4		Overcast, moderately graded and slight brightening towards the sun
5		Sky of uniform luminance
6	Partly cloudy sky	Partly cloudy sky, no gradation towards zenith, slight brightening towards the sun
7		Partly cloudy sky, no gradation towards zenith, brighter circumsolar region
8		Partly cloudy sky, no gradation towards zenith, distinct solar corona
9		Partly cloudy sky, with the obscured sun
10		Partly cloudy sky, with brighter circumsolar region
11	Clear sky	White-blue sky with distinct solar corona
12		CIE standard clear sky, low luminance turbidity
13		CIE standard clear sky, polluted atmosphere
14		Cloudless turbid sky with broad solar corona
15		White-blue turbid sky with broad solar corona

Table 2. Sky luminance distribution in tropical climate for calendar months.

Sky Type			Frequency of occurrence of standard sky types for Calendar month (%)												Overall
Type	No.	Code	Jan	Feb	Mar	Apr	May	Jun	Jul	Aug	Sep	Oct	Nov	Dec	
Overcast	1	I.1	1.72	1.91	3.18	4.00	3.92	4.45	6.51	6.88	4.11	4.37	1.34	0.84	**3.67**
	2	I.2	1.99	1.71	1.03	1.21	2.11	1.94	1.84	1.78	1.41	1.81	0.83	0.84	**1.59**
	3	II.1	2.45	2.16	2.92	6.68	7.70	8.17	8.61	9.23	8.18	6.45	2.38	2.75	**5.75**
	4	II.2	4.99	3.44	3.90	7.14	6.75	8.67	8.68	10.26	6.66	5.22	3.55	2.63	**6.15**
	5	III.1	1.06	1.22	1.40	3.53	4.60	3.85	3.37	4.43	4.24	4.15	1.59	1.31	**2.90**
	Total		**12.21**	**10.45**	**12.44**	**22.56**	**25.07**	**27.09**	**29.02**	**32.58**	**24.60**	**22.00**	**9.68**	**8.36**	**20.07**
Intermediate	6	III.2	3.80	3.64	4.44	9.32	7.62	8.52	11.41	11.66	10.03	6.41	5.01	3.10	**7.11**
	7	III.3	10.16	14.06	14.50	15.03	13.19	13.01	14.08	16.95	17.30	11.44	8.14	4.99	**12.66**
	8	III.4	13.52	22.43	19.17	7.96	8.47	9.86	8.50	7.94	9.16	10.72	10.73	6.78	**11.18**
	9	IV.2	0.53	0.68	1.00	2.50	2.52	1.73	1.20	1.89	2.49	2.69	1.71	1.05	**1.60**
	10	IV.3	2.54	2.70	3.18	6.21	5.15	3.42	2.66	5.29	5.76	3.73	2.96	2.13	**3.70**
	Total		**30.54**	**43.52**	**42.30**	**41.02**	**36.96**	**36.54**	**37.86**	**43.72**	**44.73**	**34.99**	**28.55**	**18.06**	**36.25**
Clear	11	IV.4	20.65	26.96	20.69	17.03	9.78	9.26	9.35	8.12	10.27	9.75	10.02	10.34	**13.41**
	12	V.4	3.80	1.62	2.15	3.03	5.25	3.44	3.53	2.73	4.51	3.37	5.09	5.99	**3.72**
	13	V.5	27.58	16.37	18.46	9.25	10.12	10.75	10.04	5.72	7.17	18.46	26.25	36.42	**16.42**
	14	VI.5	1.44	0.40	0.83	1.79	4.91	5.83	4.57	2.86	3.84	2.66	6.39	7.48	**3.68**
	15	VI.6	3.78	0.68	3.12	5.32	7.91	7.08	5.64	4.26	4.88	8.78	14.02	13.35	**6.45**
	Total		**57.24**	**46.03**	**45.26**	**36.42**	**37.97**	**36.37**	**33.13**	**23.70**	**30.66**	**43.02**	**61.77**	**73.58**	**43.68**

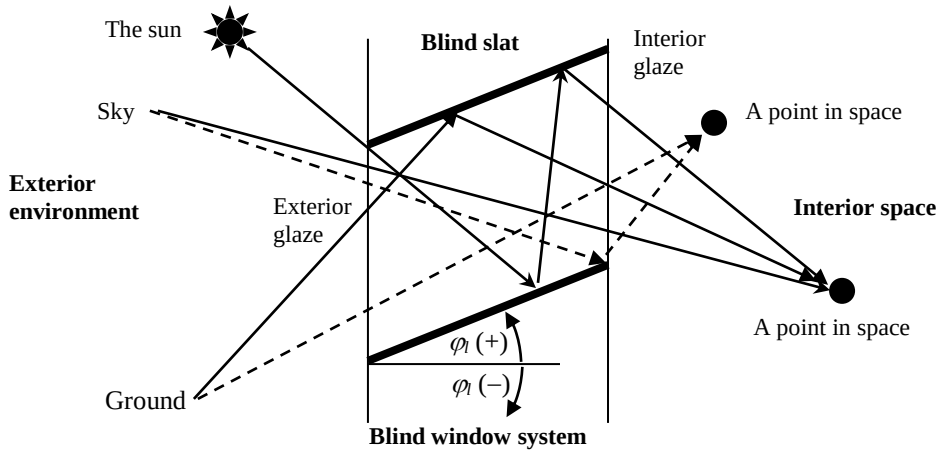

Figure 5. Daylight illuminance through the slat window.

Table 2 summarizes results of characterization of sky luminance for Bangkok in terms of frequency of the sky scans that fall into each type of standard sky distribution. Figure 4 illustrates summary result of occurrence frequency of aggregate sky types (clear, intermediate, and overcast) in each month.

In terms of aggregate sky type, Table 2 shows that overcast sky occurs 20% in a year. This varies from the lowest level at 8.4% in December, the cool month with relatively clear skies, to the highest level at 32.6% in August, the month in the midst of rainy season with relatively cloudy skies. In contrast, the table shows that clear sky occurs 43.7% in a year. This varies from 73.6% in December to 23.7% in August. The sky appears relatively clear with frequencies of occurrence from close to 60% to over 70% during November, December and January.

In Table 2, the most significant sky types are IV.4 and V.5, both are classified under clear sky. The two types together accounts for 30% of all occurrences. Type V.5 is relatively prevalent during December and January, while type IV.4 appears more frequent during January to March. Type I.1, Type I.2, Type III.1, Type IV.2, Type IV.3, Type V.4, and Type VI.5 each occurs less than 4% and together occurs less than 21% in a year. Sky type III.3 and type III.4 are two other significant types that each occurs more than 11% and together occur 24% in a year. Both types are classified under intermediate sky. Type III.3 occurs mainly during rainy season while type III.4 occurs more often during January to March, dryer period. For overcast sky, type II.1 and II.2 are prominent and together accounts for 12% in a year. From our distribution measurement, the tropical sky has distinct character with those in cold climate in terms of the prevailing prominent sky types and its occurrence frequency.

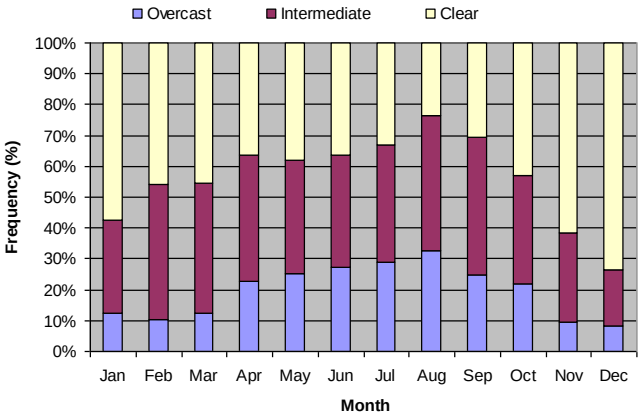

Figure 4. Occurrence frequency of each aggregate sky type for calendar month.

3. Daylight Application from the Slat Window

Section 2 demonstrates that the tropical daylight is abundant and the sky is highly luminous over a cause of year. The sun transverses overhead most of daytime and appears in all directions. To effectively utilize the tropical daylight in buildings, a simple technique is the use of shading slats to intercept the entering intense sunlight. Figure 5 exhibits a particular interesting window system that the slats are enclosed with two glazed panes. The slats can be rotated counterclockwise from the horizontal ($+\varphi_l$) and clockwise from the horizontal line ($-\varphi_l$) to regulate the daylight amount transmitted through window. For commercial buildings, the slat window is possible to be applied in various areas such as lobby hall, main office, circulating area, library, etc. The feature of the slat window is also superior to the external shading slats as they are not subject by strong wind loads.

Examine Fig. 5, the transmitted daylight through the window unit comprises the direct light from the sky and ground and the reflected light from the slat surfaces. The associated heat of the window is due to the transmitted light and the temperature difference between the outdoor and indoor air. To evaluate the slat window performance, the daylight and thermal models well documented in [24-26] were employed for the simulation. With the models, the energy consumption from lighting and air-conditioning in the room equipped with the slat window can be analyzed for identifying the suitable slat operation.

In the simulation, the modeled room was an office-like rectangular room. The room dimension was 3m wide by 15m long. The room height was 2.6m from floor to ceiling. Reflectance values of the room interior surfaces were 0.7 for ceiling, 0.5 for walls and 0.3 for floor which was typical for office rooms in commercial building. Table 3 summarizes the values of the optical properties of the glasses selected for the simulations.

The simulations were performed for the room with the 1.5m high slat window facing south. In the simulations, the slats were rotated from the angle of -50° to 50°, stepped up every 10°. The room air temperature was assumed constant at 25°C. The five-minute records of the solar radiation, daylight illuminance and ambient air condition at our daylight measuring station were used in the simulations.

3.1 Solar and thermal gains

Figure 6(a) shows the monthly average value of the incident solar radiation (E_{eS}) on the outer glass of the slat window. The value was calculated based on the working hours during 8:00-17:00. It is observed that the value of the diffuse component of the incident radiation ($E_{eS\,(d)}$) varies from 100 W/m^2 up to 160 W/m^2 over the year. For the beam component ($E_{eS\,(b)}$), the incidence value depends on the sun position relative to the window orientation. The beam incidence is none from May till August, as the sun is due north. However, its value arises in the remaining months and is highest at 245 W/m^2 in December when the sun appears in front of the window at low elevation. In the figure, the total incident radiation varies from 100 W/m^2 up to 370 W/m^2. In our study site where the sun always travels overhead and clouds present over the sky for most of the year, the diffuse radiation is dominant on the window except from November to February.

Table 3. Optical properties of the laminated glasses selected for the simulation study.

Description		Typical window	The slat window	
Glass type		Heat reflective (Single pane window)	Green-Clear (Outer glass pane)	Clear-Clear (Inner glass pane)
Solar range	Transmittance	0.06	0.41	0.75
	Reflectance	0.33	0.05	0.07
	Absorptance	0.61	0.54	0.18
Visible range	Transmittance	0.09	0.73	0.87
	Reflectance	0.32	0.07	0.07
Infrared range	Emittance	0.85	0.85	0.85

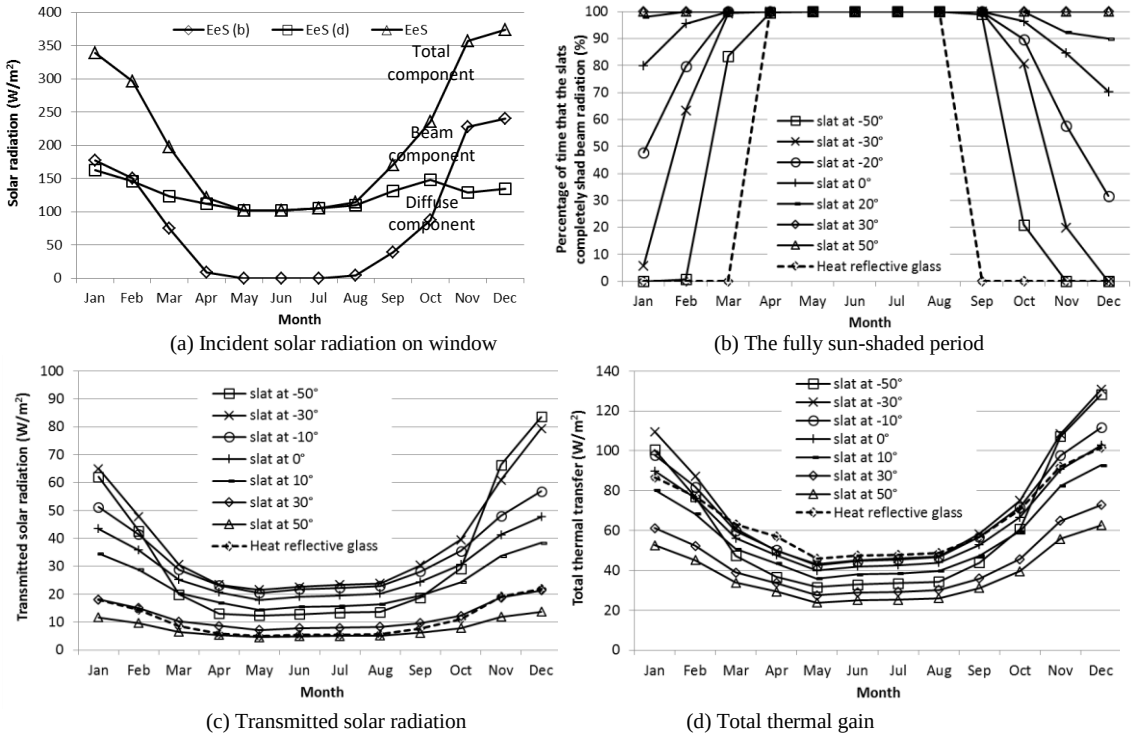

(a) Incident solar radiation on window

(b) The fully sun-shaded period

(c) Transmitted solar radiation

(d) Total thermal gain

Figure 6. Thermal simulations of the slat window facing south.

For the slat window, the slats can be tilted to a different angle to intercept the beam radiation from entering the modeled room. Figure 6(b) shows the percentage of time that the beam radiation is completely shaded by the slats. In the figure, the plot is shown for the selected slat angles of -50°, -30°, -20°, 0°, 20°, 30°, and 50°. It is observed that at 0° (horizontal position), the beam radiation is fully shaded and cannot enter the room over the whole working period from March to September (The sun stays northern from May to August). In other months, the fully sun-shaded period decreases and is shortest in December but still more than 70% of the working hours. In the figure, it is essential to rotate the slats counterclockwise exceeding 30° to ensure no direct entering of the beam radiation throughout the year.

Figure 6(b) also shows that rotating the slats clockwise from 0° (the slat angle in the negative range) sharply decreases the sun shading. None of the working hours during November-February, the slats at -50° can fully shade the beam radiation. For the glazed window with no shading device, the beam radiation enters the room for all times when the sun appears in front of the window.

Figure 6(c) shows the monthly average of the transmitted solar radiation from the slat window. It is obvious that the transmitted radiation is highly dependent on the slat angle. At 0°, the transmitted radiation is around 20 W/m^2 during April-August; approximately 20% of the incident radiation. It values is highest at an average of 48 W/m^2 in December, but this amount is only 14% of the corresponding solar incidence. The slats can effectively shade the beam component. Rotating the slats counterclockwise from 0° reduces the transmitted radiation. At these positions (slat angle), the slats intercept more the incident radiation and reflect it to the exterior. At 30°, the transmitted radiation does not exceed 22 W/m^2 on average and is comparable to that of the heat reflective glass with 6% solar transmittance.

In general, rotating the slats clockwise from 0° tends to increase the transmitted radiation. The openings between the slats that direct to the sky allow more solar radiation penetration through the openings. The incident radiation on the upper slat surface is also reflected into the room interior. In the figure, the slats at -20° maximize the solar transmission from February to October. In November, December and January, the transmitted radiation is highest at the angle of -50°. Observing Fig. 6(c), the sun-shaded area at -50° is only 20% of the window area during the three months.

Figure 6(d) shows the total thermal gain of the slat window. The gain comprises three parts of (i) the transmitted solar radiation, (ii) the inward heat flow due to the absorbed solar radiation and (iii) the heat transfer by the temperature differential between the ambient air and the room air. In most cases, the total thermal gain is largest at -20°, but it is comparable to that of the heat reflective glass. For our location where the latitude and longitude are 14.7°N and 100.5°E, in order to completely shade the beam radiation during the office hours, Fig. 6(b) shows that the slats are needed to be limited at 30° during November-February, at 10° in March and October, and at 0° from April to September. As the result of this shading, the slat window can reduce 17.2-32.7% of the total thermal gain of the heat reflective glass.

3.2 Daylight transmission

The results from the daylight simulation are next presented. Figure 7(a) shows the monthly average value of the daylight illuminances on the south facing window. The value varies from 12 klux in May to 44 klux in December and in similar pattern with the solar incidence. In Fig. 7(b), the transmitted daylight from the window is plotted against the slat angle. Influence of the slats on the daylight transmission is clearly observed. In most of the time, the transmitted daylight is highest at –20°. The sharp increase of the transmitted daylight at –50° in November-January is due to entering direct sunlight.

Figure 7(c) shows the daylight illuminance on the workplane level in January (the sun is in front of the window). The workplane daylight is high near the windowed wall and reduces exponentially along the distance to the rear wall. The slats at –30° give the highest workplane daylight for all points in the room.

Figure 7(d) shows the workplane daylight in June (the sun stays behind the window). Distinct from the previous (Fig. 7(c)), the slats at –20° give the highest workplane daylight except the area close to the windowed wall (*D/Hw*=1). This pattern actually occurs for eight month from February to October

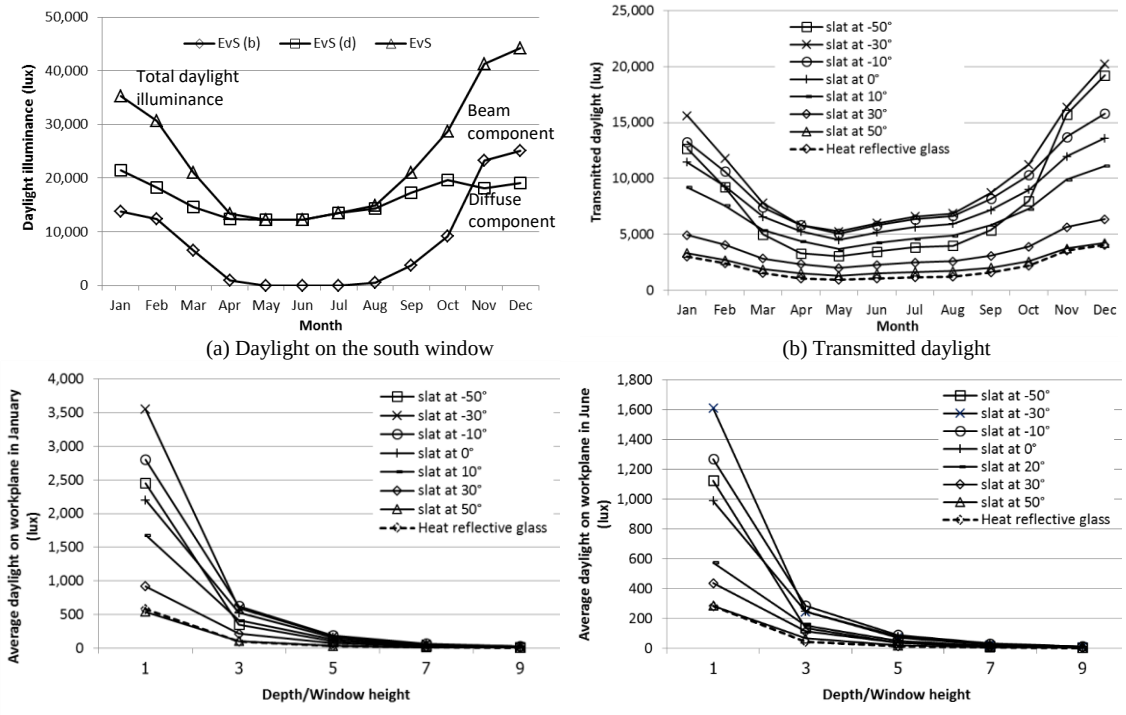

(a) Daylight on the south window

(b) Transmitted daylight

(c) Workplane daylight in January

(d) Workplane daylight in June

Figure 7. Daylight simulations of the slat window facing south.

Table 4. The luminaire and lighting power density for interior lighting in the modeled room.

Light Luminaire				E_w = (LLF) (CU) (L_f/P) (P/A)
Number of lamp			2	
Number of ballast			-	where
Total light flux (lm)			4,000.0	E_w = Target workplane illuminance
Total power (W)			44.0	LLF = Light loss factor (assumed 0.8)
Efficacy (lm/W)			90.9	CU = Coefficient of Utilization (assumed 0.65)
Workplane illuminance (lux)	800	500	300	L_f/P = Efficacy
Light power density (W/m^2)	16.9	10.6	6.3	P/A = Light power density

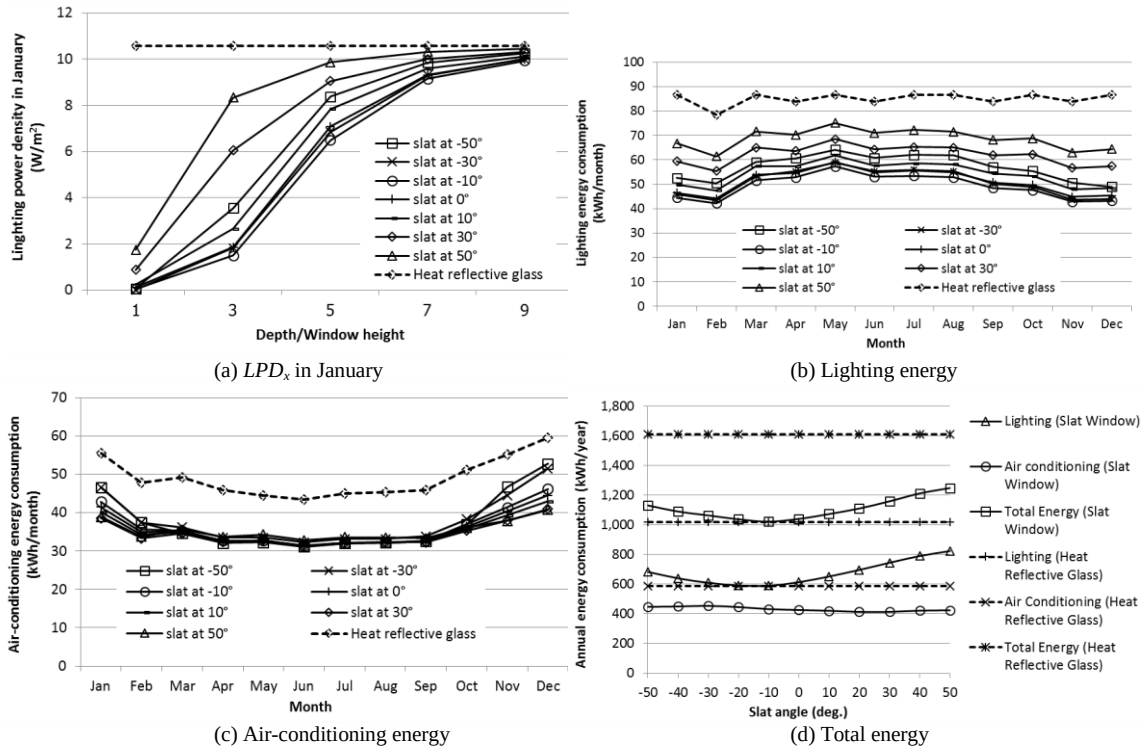

(a) LPD_x in January (b) Lighting energy

(c) Air-conditioning energy (d) Total energy

Figure 8. Energy calculations of the room with the slat window facing south (The target illuminance of 500 lux).

Examining Figs. 7(c) and (d), the daylight from the slat window in the tropics is abundant for the interior illumination. By altering of the slats from –30° to 50° the workplane daylight could be regulated from its maximum to minimum values. For the heat reflective glass, the workplane daylight illuminance is rather lower and comparable to that from the slat window at 50° (fully closed).

3.3 Energy performance

The simulated heat gain and daylight transmission were next used to evaluate the energy consumptions of the interior lighting and air-conditioning of the modeled room. It was assumed that ceiling-mounted luminaires were used to provide the uniform workplane illuminance at 0.75 m. above floor. Each luminaire was housed with two LED fluorescent lamps (22W each). Table 4 summarizes the specific information of the luminaires and its rated power calculated using the IESNA Lumen method [27]. From the table, to meet the target illuminance at 800, 500 and 300 lux, the lighting power densities (*LPD*) are at 16.9, 10.6 and 6.3 W/m^2, respectively.

With the daylighting, the dimming controller was used to regulate the light from electric lamps to supplement the daylight. The electric power was lowered linearly with the lighting reduction. For the air-conditioning, the cooling load was defined as the total sum of the dissipated heat from the electric lamps and the total thermal load from the window. The calculations postulated that the electricity supplied to lamps was finally converted to heat. As such, the heat load from the lamps was also equal to *LPD* value. The thermal load from the slat window could be calculated by the thermal model. The power requirement for the air-conditioning can be obtained by dividing the total cooling load with the air-conditioning system Coefficient of Performance (*COP*). Equation 1 expresses the monthly energy consumption of the room with the slat window (*En*) in unit kWh/year:

$$En = \left(LPD + \frac{LPD + CL \cdot (A_w / A_f)}{COP} \right) \cdot A_f \cdot H \qquad (1)$$

where *LPD* is the average lighting power density of the lighting system (in unit W/m$_{fl}^2$). *CL* is the total heat gain from the slat window (in unit W/m$_w^2$). *COP* is coefficient of performance of the air-conditioning system and assumed equal to 2.7 in the study. *H* is the working hours in each month. A_w and A_f stand for the window area and the floor area of the modeled room, respectively.

Figure 8(a) shows exemplarily the LPD_x to meet the target of 500 lux in January. The LPD_x values of *x* at D/H$_w$=1 are quite similar for all slat angles. The workplane daylight near the windowed wall was sufficient or even exceeding the target requirement. However, deep into the room (e.g. *x* at D/H$_w$=2 upto 9), more electric light was required to supplement the daylight. The LPD_x values were thus increasing and distinct among the slat angles. In the figure, the LPD_x value of the non-dimmable uniform lighting was given for benchmarking.

The average *LPD* of the modeled room was derived from the LPD_x. The lighting energy consumption was calculated in sequence. Figure 8(b) shows the monthly consumption of the electric lighting. It is observed that the consumption varied from

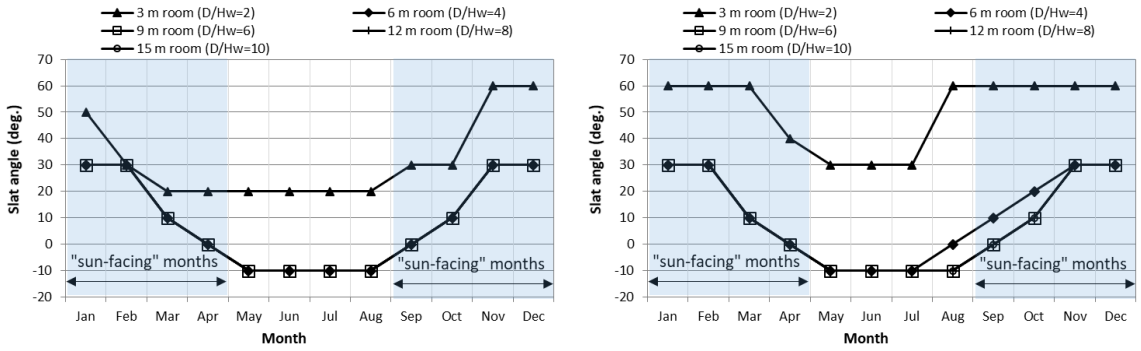

(a) Target illuminance 500 lux (b) Target illuminance 300 lux

Figure 9. The slat position of a daylight scheme to minimize energy consumption of the modeled rooms and to prevent the beam radiation entering.

Table 5. The energy consumptions of the room with slat window facing south.

Room depth (m.)	Target illuminance (lux)	Annual energy consumption (kWh/year)						Energy savings (%)		
		Room with the slat window			Room with heat reflective glass window					
		Light	Air-con	Total	Light	Air-con	Total	Light	Air-con	Total
2	300	13.6	121.7	135.3	122.5	256.0	378.5	88.9	52.5	64.3
	500	23.2	143.7	166.9	204.2	286.2	490.4	88.6	49.8	66.0
	800	29.2	179.2	208.4	326.7	331.6	658.3	91.1	46.0	68.3
4	300	30.1	176.9	207.0	245.0	301.3	546.3	87.7	41.3	62.1
	500	103.6	208.5	312.1	408.4	361.8	770.2	74.6	42.4	59.5
	800	319.7	261.8	581.5	849.5	452.6	1,302.1	62.4	42.2	55.3
6	300	112.9	212.0	324.9	360.9	344.2	705.1	68.7	38.4	53.9
	500	267.4	269.2	536.6	601.5	433.3	1,034.8	55.5	37.9	48.1
	800	528.0	365.7	893.7	962.4	567.0	1,529.4	45.1	35.5	41.6
8	300	224.5	253.3	477.8	490.1	392.1	882.2	54.2	35.4	45.8
	500	463.6	341.9	805.5	816.8	513.1	1,329.9	43.2	33.4	39.4
	800	851.5	485.5	1,337.0	1,306.9	694.6	2,001.5	34.8	30.1	33.2
10	300	341.1	296.5	637.6	612.6	437.5	1,050.1	44.3	32.2	39.3
	500	661.8	415.3	1,077.1	1,021.0	588.7	1,609.7	35.2	29.5	33.1
	800	1,172.3	604.3	1,776.6	1,633.7	815.6	2,449.3	28.2	25.9	27.5

month to month. The consumption was lowest at -10°, since the daylight from the window was maximized.

Figure 8(c) shows the air-conditioning energy consumption. The consumption was quite comparable for all angles except at 50°. The larger thermal gain from introducing more daylight could be counterbalanced by the reduced heat from the dimmed lamps. In all cases, the room with the slat window consumes less air-conditioning energy than the same room using heat reflective glazing window. This result assures no thermal penalty from the daylighting from the slat window couple with the dimmable electric lighting.

In Fig. 8(d), the annual energy consumptions of the modeled room was minimum at the angle of -10°. It should be noted that the results in the figure assume the slats were fixed at an angle throughout the year. The analysis considered only in the energy aspect with no concern of human comfort.

To further the analysis, a daylighting scheme was introduced for which the slats would be altered to minimize the room energy consumption without the direct entering of beam radiation. Under this scheme, it was expected that the occupants near the window would less experience with thermal discomfort and visual glare. Figure 9 shows the slat positions (angle) that corresponded with the lowest monthly energy consumption of the rooms with 3 m., 6 m., 9 m., 12 m. and 15 m. depths. The shaded area in the plots presents the months that the sun was in front of the window (the "sun-facing" months) and the slat angle was needed to be limited to prevent the beam radiation entering. Examining Fig. 9(a) where the target workplane illuminance was 500 lux, for the room with its depth more than four times of the window height (D/H_w>4, room depth>6m.), the daylight from the window were to be maximized for the lowest energy consumption. The slats were to be set at the limited angle that prevents the beam radiation entering in the "sun-facing" months. In the remaining months, the slats were set at –10° to introduce more daylight to minimize the energy consumption.

This practice could also be applied for the room requiring higher workplane illuminance (exceeding 500 lux). For the lower illuminance target (e.g. 300 lux), the slats are to be tilted to reduce the transmitted daylight and avoid excessive solar gain as shown in Fig. 9(b). Table 5 summarizes the annual energy consumption of the room with the slats set according to the position in Fig. 9. The consumption of the modeled office room with heat reflective glass is given for benchmarking. It can be observed that significant energy savings of 41.6-71.8% can be achieved by this simple daylighting scheme.

4. Conclusion

Daylighting has been promoted to conserve energy in buildings in Thailand. For the nationwide promotion, the present building energy code provides a scheme for accrediting the building daylight use. A station was also established to measure the daylight illuminance and the sky luminance distribution. The records could facilitate both professional design and researches on innovative daylighting technologies.

From the station records, the statistical analysis shows the tropical sky is luminous in the sense that illuminance of skylight and sunlight are high in all directions. The sky is clear or partly clear for almost 80% of the daytime. Useable daylight for daylighting

in building interior extends throughout the office hours for all year round.

Significant obstacle to the practice of daylighting is heat gain which accompanies daylight, since all commercial and public buildings are air-conditioned. Sunlight cannot be effective shaded and exacerbates heat gain and glare problems. This paper presents a practical solution of the slat window that can control the amount of useable daylight in trading off with heat gain in relatively complex situations. The performance evaluation shows that the daylighting from the slat window can conserve energy with no penalty of the excessive associated heat gain.

Reference

[1] Energy Policy and Planning Office, *Static Energy* (2018) http://www.eppo.go.th/index.php/th/energy-information/static-energy/static-electricity?orders[publishUp]=publishUp &issearch=1.

[2] Dumortier, D, Fontoynont, M, Avouac Bastie, P, *Daylight availability in Lyon* (1994) European Conference on Energy Performance and Indoor Climate in Buildings, November 24-26, 1994.

[3] Dumortier D, Evaluation of Luminous Efficacy Models According to Sky Types and Atmospheric Conditions, *Proceedings Lux Europa Conference* (1997) Amsterdam, May 11-14, 1997: pp. 1068-1080.

[4] Darula S, Kittler R, Daylighting availability after one-minute measurements for energy conscious design, Proceedings of Conference on Building Physics Symposium, October 4-6, 1995 (1995) 243-248.

[5] Chirarattananon S, Chaiwiwatworakul P, Pattanasethanon S, Daylight availability and models for global and diffuse horizontal illuminance and irradiance for Bangkok, *Renewable Energy* 26/1 (2002) 69-89.

[6] Ineichen P, Molineaux B, Perez R, Sky Luminance data validation: Comparison of seven models with four data banks, *Solar Energy* 52/4 (1994) 337-346.

[7] Littlefair PJ, A comparison of sky luminance models with measured data from Garston, United Kingdom, *Solar Energy* 53/4 (1994) 315-322.

[8] Muneer T, Evaluation of the CIE overcast sky model against Japanese data, *Energy and Buildings* 27/2 (1998) 175-177.

[9] Chirarattananon S, Chaiwiwatworakul P, Distributions of sky luminance and radiance of north Bangkok under standard distributions, *Renewable Energy* 26/8 (2007) 1328-1345.

[10] Kischkoweit-Lopin M, An overview of daylighting systems, *Solar Energy* 73/2 (2002) 77-82.

[11] Mashaly IA, Nassar K, Haggar S, Mathematical model for designing a light redirecting prismatic panel, *Solar Energy* 159 (2018) 638-649.

[12] James PAB, Bahaj AS, Holographic optical elements: Various principles for solar control of conservatories and sunrooms, *Solar Energy* 78/3 (2005) 441-454.

[13] Linhart F, Wittkopf SK, Scartezzini JL, Performance of anidolic daylighting systems in tropical climates – Parametric studies for identification of main influencing factors, *Solar Energy* 84/7 (2010) 1085-1094.

[14] Leung TCY, Rajagopalan P, Fuller R, Performance of a daylight guiding system in an office building, *Solar Energy* 94 (2013) 253-265.

[15] Chaiwiwatworakul P, Chirarattananon S, A double-pane window with enclosed horizontal slats for daylighting in buildings in the tropics, *Energy and Buildings* 62 (2013) 27-36.

[16] Fathoni AM, Chaiwiwatworakul P, Mattanant V, Energy analysis of the daylighting from a double-pane glazed window with enclosed horizontal slats in the tropics, *Energy and Buildings* 128 (2016) 413-430.

[17] Chirarattananon S, Chedsiri S, Renshen L, Daylighting through light pipes in the tropics, *Solar Energy* 69/4 (2000) 331-341.

[18] Taengchum T, Chirarattananon S, Exell RBH, Chaiwiwatworakul P, Tracing of daylight through circular light pipes with anidolic concentrators, *Solar Energy* 110 (2014) 818-829.

[19] Mangkuto RA, Feradi F, Putra RE, Atmodipoero RT, Favero F, Optimisation of daylight admission based on modifications of light shelf design parameters, *Journal of Building Engineering* 18 (2018) 195-209.

[20] Edmonds IR, Performance of laser cut light deflecting panels in daylighting applications, *Solar Energy Materials and Solar Cells* 29/1 (1993) 1-26.

[21] Piccolo A, Marino C, Nucara C, Pietrafesa M, Energy performance of an electrochromic switchable glazing: Experimental and computational assessments, *Energy and Buildings* 165 (2018) 390-398.

[22] Chirarattananon S, Chaiwiwatworakul P, Hien VD, Rakkwamsuk P, Kubaha K, Assessment of energy savings from the revised building energy code of Thailand, *Energy* (2010) 35/4 1741-1753.

[23] International Commission for Illumination, *International Standard ISO 15469:2004(E)/CIE S011/E: 2003, Spatial distribution of daylight-CIE standard general sky* (2004) International Organization for Standardization and International Commission for Illumination.

[24] Chaiwiwatworakul P, Chirarattananon S, Rakkwamsuk P, Application of automated blind for daylighting in tropical region, *Energy Conversion and Management* 50/12 (2009) 2927-2943.

[25] Chaiwiwatworakul P, Chirarattananon S, A double-pane window with enclosed horizontal slats for daylighting in buildings in the tropics, *Energy and Buildings* 62 (2013) 27-36.

[26] Fathoni AM, Chaiwiwatworakul P, Mattanant V, Energy analysis of the daylighting from a Double-pane Glazed Window with Enclosed Horizontal Slats in the Tropics, *Energy and Buildings* 128 (2016) 413-430.

[27] IES, Committee on Calculation Procedures, *IES recommended practice for the lumen method of daylight calculations. IES RP-23-1989* (19891) New York: Illuminating Engineering Society.

